WATER RESOURCES RESEARCH, VOL. 34, NO. 5, PAGES 1035–1050, MAY 1998

In situ estimation of soil hydraulic functions using a multistep soil-water extraction technique

M. Inoue
Arid Land Research Center, Tottori University, Tottori, Japan

J. Šimunek
USDA Salinity Laboratory, Riverside, California

J. W. Hopmans and V. Clausnitzer
Hydrology Program, University of California, Davis

Abstract. Estimation of the retention and unsaturated hydraulic conductivity functions is essential to effectively provide input for water flow and transport simulation and prediction. A parameter optimization procedure is shown as a promising tool to estimate inversely these hydraulic function parameters from transient soil matric potential and cumulative soil solution extraction measurements. Sensitivity analyses from synthetic data generated from forward numerical model simulations showed that optimum tensiometer locations will depend on soil type. Experiments were carried out in both a laboratory column (Columbia sandy loam) and in the field (Yolo silt loam). In both cases a series of vacuum extraction pressures was applied to a ceramic soil solution sampler, and cumulative soil solution extraction volume and matric potentials at various positions near the extraction device were monitored as the soil solution was extracted. In the laboratory a zero-flux boundary condition was maintained at the bottom of the column, whereas matric potential measurements were used in the field to define the lower boundary. In both the field and laboratory experiments, flow at the upper boundary was zero. Cumulative extraction volume and matric potential data were included in the objective function to be minimized to estimate the hydraulic function parameters. We determined that the optimized solution was sensitive to the contact between the ceramic ring and the surrounding soil. By also optimizing the hydraulic resistance of the ceramic ring of the extraction device, optimization improved the fit between measured and optimized flow variables. Comparison of the optimized with the independently measured hydraulic functions indicated that the in situ estimation using a multistep extraction procedure can provide accurate soil hydraulic data.

1. Introduction

As the concern for a safe, clean environment and high groundwater quality increases, the importance of an accurate soil physical description of the combined unsaturated-saturated porous system is increasingly recognized in the fields of environmental engineering and groundwater hydrology. Moreover, accurate soil physical data is required for the suite of increasingly available agrohydrological simulation models and in the modeling of land surface processes to simulate the exchange of sensible and latent heat between the soil and atmosphere. With this wider interest the spatial scale of interest has shifted to larger dimensions. Soil hydraulic and transport characterization is needed for soil-water systems as large as a watershed and for depths extending from the rooting zone to the groundwater. This trend in larger spatial scales brings with it the need to consider soil heterogeneity within the considered system. Therefore methodologies need to be developed that allow for a rapid and accurate characterization of the soil physical properties and its spatial variability.

Currently, many laboratory and field methods exist to determine the highly nonlinear soil hydraulic functions of the soil water retention and unsaturated hydraulic conductivity curves. Most methods require restrictive initial and boundary conditions, which make measurements time consuming, range restrictive, and expensive. Excellent reviews have been published by *Klute and Dirksen* [1986], *Klute* [1986], and *Green et al.* [1986]. *Dirksen* [1991] discusses the application of parameter estimation by the inverse solution technique as a viable alternative to other traditional laboratory methods for soil hydraulic characterization. The speed at which results for a large number of soil samples can be obtained via multiplexing of sensors, and recent developments in improved TDR and pressure sensors make this inverse technique a viable alternative. The parameter optimization method is especially advantageous since single experiments can yield simultaneous estimates of the soil water retention and unsaturated hydraulic conductivity functions.

Since the early 1970s the inverse problem of parameter identification for distributed numerical models has been applied in groundwater hydrology and field petroleum engineer-

Paper number 98WR00295.
0043-1397/98/98WR-00295$09.00

ing. *Yeh* [1986] presented an excellent review of the inverse problem as a parameter identification procedure in groundwater hydrology. Its application to the vadose zone started later and has been limited mostly to parameter estimation of soil hydraulic properties. Parameter estimation, as defined in this study, involves the indirect estimation of soil hydraulic functions by numerical solution of the governing flow equation and subsequent comparison of the numerical solution with experimental data. In this procedure, soil hydraulic properties are assumed to be described by an analytical model, with as yet unknown parameter values. An experiment is then set up under controlled conditions with prescribed initial and boundary conditions. During the experiment, one or more flow-controlled variables are measured. Subsequently, the Richards equation is solved numerically using the hydraulic functions with initial estimates for their parameters. These parameters are then optimized by minimization of an objective function containing the sums of squared deviations between observed and predicted flow variables, using repeated numerical simulations of the flow process. This iterative inversion of the flow equation is in contrast to direct inversion techniques as used in analytical solutions.

Among the first to suggest the application of computer models to estimate soil hydraulic parameters were *Whisler and Watson* [1968], who reported on estimation of the saturated conductivity of a draining soil by matching observed and simulated drainage. The pressure plate outflow method was introduced by *Gardner* [1956], in which an initially saturated soil was subjected to a series of step increases in air pressure with the drainage or outflow measured after each pressure step increase. Given specific assumptions, the analytical solution yields the soil diffusivity as a function of water content. *Doering* [1965] improved the outflow method by proposing a one-step experiment, thereby achieving considerable time savings without loss in accuracy. Other modifications were introduced more recently by *Valiantzas and Kerkides* [1990], who extended the outflow method to simultaneous determination of soil water retention and unsaturated hydraulic conductivity using the *Brooks and Corey* [1966] formulation of the soil hydraulic properties.

Although the application of the inverse approach to the outflow method appeared promising, problems were encountered with the nonuniqueness of the optimized parameters [*van Dam*, 1990]. Nonuniqueness leads to more than one set of parameters, yielding minimum values for the objective function determined by local minima, or by the same global minimum at more than one point in the parameter space [*Carrera and Neuman*, 1986b]. The study of nonuniqueness problems has lead to many investigations on the type of experiments, and the measured flow variables that need to be included in the objective function.

Kool et al. [1985] and *Parker et al*. [1985] were the first to apply the inverse approach by numerical solution of the Richards equation for a transient one-step outflow experiment. They concluded that uniqueness problems were minimized if the experiment were designed to cover a wide range in water contents. *Kool and Parker* [1988] discussed the advantage of including tensiometric data simultaneously with the outflow measurements in the inverse approach from a hypothetical infiltration and redistribution experiment. In addition, the analysis of the objective function by *Toorman et al*. [1992] indicated that uniqueness problems were minimized if soil water pressure head data were included in the objective function of a transient one-step outflow experiment. To circumvent the need for additional soil water pressure measurements in the outflow experiment, *van Dam et al*. [1994] conducted outflow experiments in which the pneumatic pressure was increased in several smaller steps. Their work for a loam soil showed that the outflow data of a multistep experiment contain sufficient information for unique estimates of the soil hydraulic functions. The experimental work by *Eching and Hopmans* [1993] and *Eching et al*. [1994] showed how the multistep method, in combination with automated soil water pressure measurements during drainage of the soil core, resulted in unique parameter values for the optimized soil hydraulic functions for four different textured soils.

The most recent applications of the parameter optimization approach for the estimation of soil hydraulic properties include two-dimensional hypothetical experiments and flow simulations. For example, *Šimunek and van Genuchten* [1996] demonstrated that tension disc permeameter experiments complemented with soil matric potential data guarantee numerical convergence and uniqueness of the optimized parameters. In their subsequent study, *Šimunek and van Genuchten* [1997] showed that additional soil matric potential data are not needed, provided the infiltration experiment is carried out with several consecutive tensions and the initial and final water contents below the tension disc are known. *Gribb* [1996] used hypothetical infiltration data from a modified conepenetrometer to indirectly estimate the soil hydraulic functions. The cone-shaped device included a porous filter near the cone through which water was injected in the unsaturated soil, and two tensiometer rings above the filter. As the volume of infiltrated water is monitored, the soil water matric potential response was measured by the two tensiometer rings.

While a majority of applications of the parameter estimation technique was only for laboratory studies, the objective of this paper is mainly to demonstrate the potential application of soil water extraction method to estimate soil water retention and unsaturated hydraulic conductivity parameters in the field. The feasibility of the vacuum extraction technique is first demonstrated from numerically generated data. Subsequently, the parameter estimation technique was applied to laboratory and in situ field data.

2. Materials and Methods

2.1. Water Flow Theory

The proposed method is based on the premise that the soil's hydraulic properties can be estimated from the measurement of extracted soil water volume and soil water potential values at various locations as a function of time. This is done by applying a number of vacuum increments to a ceramic soil water extraction device. Although the experiments will occur spatially in three dimensions, we can assume axial symmetry for isotropic soils, which reduces the Richards equation to two dimensions, which for a rigid porous media can be written as

$$C\frac{\partial h}{\partial t} = \frac{1}{r}\frac{\partial}{\partial r}\left(rK\frac{\partial h}{\partial r}\right) + \frac{\partial}{\partial z}\left(K\frac{\partial h}{\partial z}\right) + \frac{\partial K}{\partial z} \qquad (1)$$

where C is the water capacity $[L^{-1}]$, h is the soil matric potential $[L]$, K is the unsaturated hydraulic conductivity $[L\ T^{-1}]$, r is the radial coordinate $[L]$, z is the vertical coordinate (positive upward) $[L]$, and t is time $[T]$. Equation (1) was solved with the Galerkin finite element method based

on the mass conservative iterative scheme proposed by *Celia et al*. [1990]. An example of a typical flow domain with the applied finite element mesh including geometry notation and locations of matric potential measurements (T_1 through T_3) is presented in Figure 1. The mesh size of the triangular elements gradually increases from 0.15 cm for the porous cup to 1.3 cm in the soil. The smaller size in and near the porous cup is required since it is there that the largest potential gradients occur.

Boundary and initial conditions for which (1) was solved are dependent on the specific experiment, but they can be generally defined as

$$h(r, z, t) = h_i(z) \qquad t = t_0,\ 0 < r < R \tag{2}$$

Lab

$$q(r, z, t) = 0 \qquad z = 0,\ 0 < r < R,\ t_0 < t < t_{\text{end}} \tag{3a}$$

or

Field

$$h(r, z, t) = h_{lb} \quad z = -55 \text{ cm},\ 0 < r < R,\ t_0 < t < t_{\text{end}} \tag{3b}$$

Lab

$$h(r, z, t) = h_{ex} \quad r = r_i(2.70 \text{ cm}),\ 16.5 < z < 19.5 \text{ cm} \tag{4}$$

Field

$$h(r, z, t) = h_{ex} \qquad r = r_i(2.70 \text{ cm}),\ -11.5 < z < -8.5 \text{ cm}$$

$$q(r, z, t) = 0 \quad \text{remaining boundaries},\ t_0 < t < t_{\text{end}} \tag{5}$$

where $r = R$ denotes the radius of the flow domain [L], the ordinate $z = 0$ is placed at the bottom or top of the flow domain for lab and field experiments (see Figure 1), respectively; t_0 and t_{end} correspond to the beginning and end of the extraction experiment [T], respectively; and r_i is the inside radius of the extraction device [L]. Equations (3a) and (3b) specify the bottom boundary condition for the lab and field experimental setups, respectively; with h_{lb} [L] being the measured pressure head at the bottom of considered transport domain. Equation (4) represents the applied suction h_{ex} [L] in the extraction sampler. In solving (1), subject to conditions (2) through (5), the unsaturated hydraulic properties are defined by [*van Genuchten*, 1980; *Mualem*, 1976]

$$S_e = \frac{\theta(h) - \theta_r}{\theta_s - \theta_r} = \frac{1}{(1 + |\alpha h^n|)^m} \tag{6}$$

and

$$K(\theta) = K_s S_e^{1/2}[1 - (1 - S_e^{1/m})^m]^2 \qquad h < 0 \tag{7}$$

$$K(\theta) = K_s \qquad h \geq 0 \tag{8}$$

In expressions (6)–(8), S_e is the effective saturation [–]; θ_r and θ_s denote the residual and saturated volumetric water contents [–], respectively; α [L^{-1}] and n [–] ($m = 1 - 1/n$) are empirical parameters; and K_s is a fitted saturated hydraulic conductivity [$L\ T^{-1}$], not necessarily equivalent to an independently measured saturated hydraulic conductivity. Since the ceramic ring is considered part of the porous system in the numerical simulations, parameter values were chosen such that the ceramic remained fully saturated over the imposed range of h_{ex}.

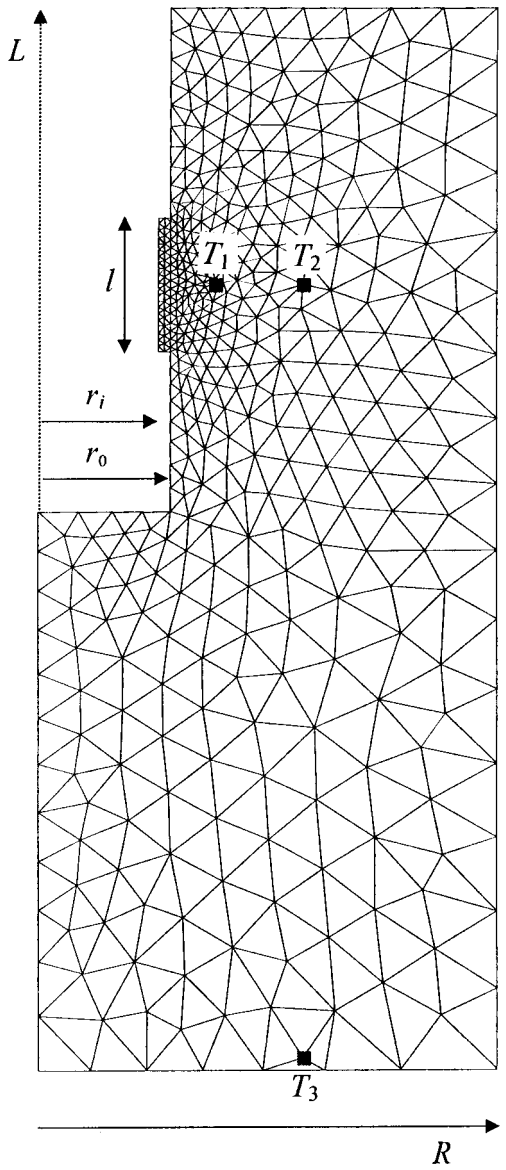

Figure 1. Finite element mesh and geometry notation for flow domain of hypothetical and laboratory experiments.

2.2. Parameter Optimization

Parameters in (6)–(8) were estimated from maximization of the log likelihood function [*Bard*, 1974], which includes differences between the observed and predicted flow variables. Assuming measurement errors to be independent with zero mean, the parameter optimization procedure is equivalent to minimization of a weighted, least squares problem, which is cast in an objective function, OF(**b**), with **b** denoting the vector containing the optimized parameters

$$\text{OF}(\mathbf{b}) = \sum_{j=1}^{m} \left(w_j \sum_{i=1}^{n_j} w_{i,j} [q_j^*(t_i) - q_j(t_i, \mathbf{b})]^2 \right) \tag{9}$$

where j represents the different sets of measurements (cumulative extraction volume, matric potential head at different locations, or water volume in flow domain), n_j is the number of measurements within a particular set, $q_j^*(t_i)$ are measurements of type j at time t_i, $q_j(t_i, \mathbf{b})$ are the corresponding model

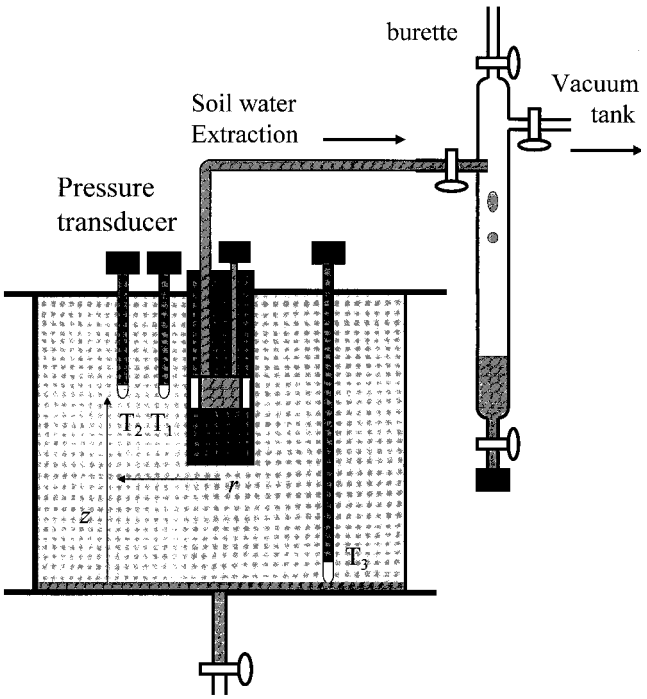

Figure 2. Layout of laboratory experiment.

predictions using the parameters in **b**, and w_j and $w_{i,j}$ are weighting factors associated with data type and data point, respectively. Assuming that measurement errors for all pressure transducers were identical, $w_{i,j}$ was set equal to 1 for all pressure measurements, whereas the water volume measurements were given a weighting factor of 10. Differences in weighting between data types, as caused by differences in magnitudes and their number n_j, were minimized by division of each data point by the variance of the measurements of data type j and by n_j [*Clausnitzer and Hopmans*, 1995]

$$w_j = \frac{1}{n_j}\frac{1}{\sigma_j^2} \tag{10}$$

where σ_j and n_j denote the standard deviation and the number of data of the j-type measurements, respectively. Thus OF(**b**) is equal to the weighted average squared deviation between simulated and measured flow variables. An effective method to minimize (9), which uses a combination of the Newton and steepest descent method, was proposed by *Marquardt* [1963]. Details of this procedure have been given by *Kool et al*. [1987] and *Šimunek and van Genuchten* [1996]. It suffices to state that the Levenberg-Marquardt method is a standard method in nonlinear least squares fitting which, in addition to the sum of squared residuals of (9), also provides confidence intervals for the optimized parameters.

2.3. Sensitivity Coefficients

An experiment must be designed such that direct information is available for the least sensitive parameters, thereby eliminating them from the optimized parameter set or providing good initial well-constrained estimates. Choice of data type and their measurement in space and time should be based on a sensitivity analysis as well, so that their sensitivity to the optimized parameters is maximum [*Šimunek and van Genuchten*, 1996]. A review on ill-posedness and error analysis of the optimized parameters has been given by *Kool and Parker* [1988], *Yeh* [1986], and *Carrera and Neuman* [1986a, b].

The sensitivity coefficients ($s_{i,j}$) for the hypothetical experiments described below were calculated from [*Šimunek and van Genuchten*, 1996]

$$s_{i,j} = 100 b_j \frac{\partial q_i}{\partial b_j} \tag{11}$$

where $s_{i,j}$ denotes the change of measurement variable q_i relative to a 1% change of the parameter b_j, and the partial derivative term is estimated from

$$\frac{\partial q_i}{\partial b_j} = \frac{q_i(\mathbf{b} + \Delta \mathbf{b} e_j) - q_i(\mathbf{b})}{\Delta b_j} \tag{12}$$

where e_j is the jth unit vector, and $\Delta b_j = 0.01 b_j$. Equation (11) allows comparison of sensitivities between parameters, independent of their unit or absolute value.

The time-averaged sensitivity, $S(r, z, b_j)$, and maximum sensitivity, $S_{\max}(r, z, b_j)$, of the measured soil water potential values to each of the four parameters b_j were calculated for the whole flow domain from

$$S(r, z, b_j) = \frac{1}{(t_0 - t_{\text{end}})} \int_{t_0}^{t_{\text{end}}} s_{h,j}(r, z, t)\, dt \tag{13a}$$

and

$$S_{\max}(r, z, b_j) = \text{Maximum } \{s_{h,j}(r, z, t, b_j)\}\ t_0 < t < t_{\text{end}} \tag{13b}$$

where $S_{h,j}$ is the sensitivity of the soil matric potential to parameter b_j calculated for each node of the flow domain using (10). This information allows us to evaluate the importance of tensiometer location in multistep extraction experiments.

2.4. Numerical Experiments

Soil water extraction accompanied by soil water potential response was simulated using forward simulations using the two-dimensional flow model HYDRUS-2D of *Šimunek et al*. [1996]. The dimensions of the flow domain were $R = 10.4$ cm and $L = 24.3$ cm, where L is the coordinate of the soil surface [L] (Figure 1). Dimensions and instrument locations were identical as used in the subsequent laboratory experiment. The 3.0-cm-long ceramic ring of the extraction device (l) was inserted in the center of the soil column ($r = 0$), with its center located 6.3 cm below the soil surface (d). Three hypothetical tensiometers were installed (see also in Figure 2) at the following positions: $r = 4.0$ cm and $z = 18$ cm (T_1); $r = 6.0$ cm and $z = 18$ cm (T_2); and $r = 6.0$ cm and $z = 0.3$ cm (T_3). Forward hypothetical simulations were done using a sandy loam and silt soil, for which *Carsel and Parrish* [1988] presented the hydraulic parameters. Parameter values are presented in Table 1. The three soils represent a wide range in soil hydraulic properties, so that simulations for likely soil types could be evaluated from these data. As the initial condition, hydraulic equilibrium was assumed with a soil water potential of 0 cm at the bottom of the soil column, corresponding with a soil water potential of −24.3 cm at the soil surface. The following vacuum steps were applied to the extraction device: $h_{\text{ex}} = -30$ cm ($0 < t < 60$ h), $h_{\text{ex}} = -60$ cm ($60 < t < 120$ h), $h_{\text{ex}} = -120$ cm ($120 < t < 240$ h), $h_{\text{ex}} = -240$ cm ($240 < t < 360$ h), and $h_{\text{ex}} = -480$ cm ($360 < t < 600$ h).

Soil matric potential at the three hypothetical locations (h_1, h_2, and h_3; or q_j, $j = 1$, 2, and 3 in (9)) and cumulative extraction volume (Q, q_4 in (9)) were simulated for these soil types for the given initial and boundary conditions. In the next step the parameters α, n, θ_r, and K_s were optimized from discrete values of the simulated Q and soil matric potential values h_1 through h_3 by inverse solution using identical initial and boundary conditions. The saturated water content, θ_s, was assumed to be known. Four sets of initial parameter values for each optimization were taken from *Carsel and Parrish* [1988] using parameters for the sandy loam, loam, silt, and clay (true values for sand); sand, loam, silt loam, and clay (silt); and sand, sandy loam, silt, and clay (loam), which combined include the whole range of possible parameter values. The correspondence of each of the four sets of final parameter values with their true values used in the forward simulations yields information on the uniqueness of the parameters for the given experimental conditions and soils.

2.5. Laboratory Experiment

The flow regime was identical to that used in the numerical experiments. The extraction device consists of a 6.0-cm-outside-diameter (OD) PVC pipe with a total vertical length of 11.5 cm, with a 3-cm-long porous ceramic ring (Soil Moisture Equipment Corporation) glued in the tube, 6.3 cm from the top. The inside (r_i) and outside (r_0) radiuses of the ceramic ring were 2.70 and 3.02 cm, respectively. Tensiometers were constructed by cementing a 1-cm-long 0.635-cm-OD ceramic cup (Soil Moisture Equipment Corporation) to 0.63-cm-OD acrylic tubing. After filling with water, a pressure transducer (Omega Technologies Corporation) was connected to the water-filled tubing using a short piece of tygon tubing. Transducers were connected to a 21X data logger using an AM416 multiplexer (Campbell Scientific Corporation), providing soil matric potential measurements with an accuracy of about 2 cm. The K_s value for the ceramic ring material, K_{cer} [LT^{-1}], was independently measured by imposing a pressure difference across the ring, while submerged in water. The Darcy equation in radial coordinates was used to solve for K_{cer} analytically, leading to

$$K_{cer} = \frac{Q \ln \frac{r_0}{r_i}}{2\pi l (h_{out} - h_{in})} \quad (14)$$

where Q is the steady state volumetric flow rate [L^3 T^{-1}] extracted through the ring of length l [L], and h_{out} and h_{in} denote the soil matric potential values at the outside and inside of the ring [L] at radial distances of r_0 and r_i from the center of the ring [L] (Figure 1), respectively. Replicated measurements yielded $K_{cer} = 8.334 \times 10^{-4}$ cm h^{-1}.

A schematic of the laboratory experiment, which includes the burette assembly for vacuum extraction and the boundary conditions, is presented in Figure 2. The soil used was a Columbia fine sandy loam. The soil was air dried, sieved through a 2-mm screen, and packed uniformly to a dry bulk density of 1.46 g/cm^3 in the soil column with porous plastic on the bottom. The soil was saturated from the bottom by applying a slight positive pressure to the water. After saturation, hydraulic equilibrium was established by applying a water potential of about 0 cm at the bottom of the column using a Mariotte device for 6 days. At this time, drainage rate was zero and tensiometer measurements indicated a zero total soil water potential gradient, with a soil matric potential of -3.3 cm at $z = 0.3$ cm (T_3) and -21 cm at $z = 18$ cm (average of T_1 and T_2). Therefore, assuming hydraulic equilibrium, h_i is -3.0 cm at the bottom and linearly decreases to -27.3 cm at the top of the column. Measurement accuracy of the tensiometer readings was determined from separate calibration of each transducer and varied between ± 1–2 cm. A 0.7-cm-thick PVC plate to prevent evaporation of the soil during the extraction experiment covered the column.

Table 1. Soil Hydraulic Parameters for Selected Textural Classes

Soil Type	θ_s	θ_r	α, cm^{-1}	n	K_s, cm h^{-1}
Sand	0.43	0.045	0.145	2.68	29.7
Sandy loam	0.41	0.065	0.075	1.89	4.42
Loam	0.43	0.078	0.036	1.56	1.04
Silt loam	0.45	0.067	0.02	1.41	0.45
Silt	0.46	0.034	0.016	1.37	0.25
Clay	0.38	0.068	0.008	1.09	0.02

Carsel and Parish [1988].

The water-filled chamber of the extraction device was connected to a burette by tygon tubing. While applying vacuum to the air phase in the burette, the extracted soil water flows into the burette with the pressure of the inflow end equal to the applied vacuum. The volume of extracted water was measured both manually and using a pressure transducer in the bottom of the burette (Figure 2). A film of oil to prevent water loss by evaporation covered the water in the burette. The measurement error of the burette readings was about 0.2 mL. While vacuum was applied to the extraction device, the water pressure in the chamber was measured simultaneously using a tensiometer connected to a pressure transducer. Average vacuum steps (as measured in the chamber of the extraction device) were $h_{ex} = -35$ cm ($0 < t < 25$ h), $h_{ex} = -65$ cm ($25 < t < 73$ h), $h_{ex} = -125$ cm ($73 < t < 217$ h), $h_{ex} = -240$ cm ($217 < t < 339$ h), and $h_{ex} = -480$ cm ($339 < t < 605$ h).

From weight measurements of the column at the end of the extraction experiment at 605 h (t_{end}), after oven drying, and at the initial time (t_0), values for column average volumetric water content and dry soil bulk density were calculated. The dry bulk density was 1.46 g cm^{-3}, whereas the column-average volumetric water content values at t_0 and t_{end} were 0.37 and 0.22 cm^3 cm^{-3}, respectively. The volumes of water (cm^3) corresponding with these two water content values (2939 and 1758 mL) were included in the objective function, thereby insuring that the initial and final conditions of the experiment and simulation model were identical.

The soil water retention function was independently determined from a multistep outflow experiment [*Eching and Hopmans*, 1993] for the same soil with a slightly lower bulk density of 1.42 g cm^{-3}. The soil was air dried and sieved, and a 216-cm^3 sample was packed in a 6.4-cm-diameter core. Subsequently, the soil was saturated with water in a Tempe pressure cell. Various air pressure increments were applied to drain the sample, during which the soil matric potential in the center of the core and total drainage volume was measured.

2.6. Field Experiment

A detailed overview of the field experiment is presented in Figure 3. The field soil is a Yolo silt loam with an approximate

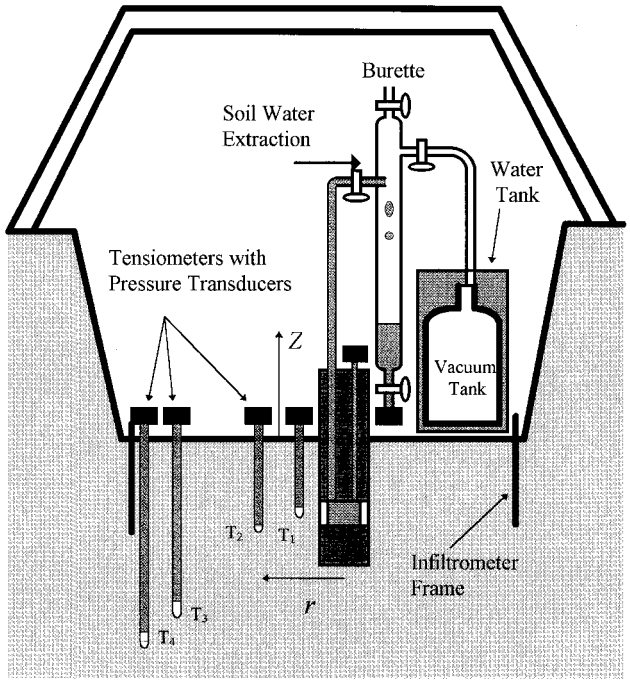

Figure 3. Experimental setup of in situ multistep extraction experiment.

clay content of 22% [*Eching and Hopmans*, 1993]. Soil was excavated to a depth of 60 cm and leveled. The ceramic extraction device (OD 6 cm) was installed in the center of the plot ($r = 0$) into a hole of 5.1. cm OD, created beforehand with a soil sampler, with the center of the ceramic ring at $z = -10$ cm depth. The ceramic extraction device was wetted before installation to insure the best possible contact between the soil and ceramic. Similar tensiometers as applied in the laboratory experiment were installed at the following positions: $r = 4.0$ cm and $z = -10$ cm (T_1); $r = 6.0$ cm and $z = -15$ cm (T_2); $r = 20.0$ cm and $z = -40$ cm (T_3); and $r = 20$ cm and $z = -55$ cm (T_4). Vacuum was applied to the burette using a vacuum tank, which was evacuated at a predetermined vacuum for each of the solution extraction step increments. The plot was covered with a shelter to minimize temperature fluctuations which would influence the vacuum in the tank.

The 1.2 m × 1.2 m square plot was ponded with a constant head of 0.5 cm water for about 3 days until the steady state infiltration rate was 1 cm h^{-1} (decreased from 1.3 to 0.85 cm h^{-1} during the 3-day period). After 3 days the total water potential gradient ($H = h + z$), dH/dz, between T_3 and T_4 was approximately 1 cm cm^{-1}. Subsequently, the plot was covered by a plastic sheet to prevent soil evaporation. The soil was allowed to drain for a period of 46.5 h at which time the total head gradient was about 0.3 cm cm^{-1}. After the 46.5 hours of free drainage, the first vacuum extraction step was applied ($h_{ex} = -195$ cm for $46.5 < t < 71.2$ h). Subsequent vacuum steps were $h_{ex} = -415$ cm for $71.2 < t < 93.0$ h, and $h_{ex} = -685$ cm for $93.0 < t < 120$ h.

From core samples at the 60-cm soil depth, measured saturated volumetric water content was 0.56 cm^3 cm^{-3} and K_s varied between 2.12 and 2.94 cm h^{-1}. Dry bulk density of these samples varied between 1.27 and 1.35 g cm^{-3}. Time zero for the computer simulations was at the conclusion of the infiltration test. During the extraction experiment (December 4–9, 1995), soil samples representing the 8-cm soil depth were collected and volumetric water content was determined from oven drying. These volumetric water content data were matched with soil water potential values of the T_1 tensiometers, resulting in the following $\theta - h$ (cm) points: (0.39, −94), (0.36, −133), and (0.35, −149) (Figure 10a). Also these three independently measured soil water retention points were included in the OF (9). In addition to the tensiometers used to measure response to soil water extraction, additional tensiometers were installed at depths of 8 and 20 cm, at distances of more than 20 cm away from the ceramic extraction device. These matric potential measurements were not influenced by water extraction, and together with the 40- and 55-cm-deep tensiometers characterized the draining of the soil profile by gravity forces. Therefore these matric potential measurements in combination with water content measurements using a neutron probe at depths of 25, 40, 55, and 70 cm were used to obtain additional independent estimates of in situ $\theta(h)$ and $K(\theta)$ data using the instantaneous profile method [*Green et al.*, 1986].

3. Results and Discussion

3.1. Numerical Experiments

Parameter optimization results for parameters α, n, θ_r, and K_s (θ_s) of the silt, sand, and loam using four initial parameter estimates are presented in Table 2. The daggers in the last column indicate optimized parameter values that are within 1% of the true values. Already, it must be pointed out that the parameter optimization method is tested for extreme conditions; that is, initial parameters were selected from the whole range of soil textural classes to test convergence for any of the three soil types. In reality, one would select as an initial estimate a parameter set close to the expected final parameter values. In almost all optimizations for which parameter values were different from their true values by more than 1%, simulated cumulative extraction volume and soil matric potential values agreed well with the true values. In such cases the inverse solution converged to a local minimum with a value of

Table 2. Parameter Optimization Results for Synthetic Cases

Initial Estimates*	Final Estimates				
	θ_r	α, cm^{-1}	n	K_s, cm h^{-1}	OF
			Sand		
Sandy loam	0.050	0.136	2.686	20.97	0.16e-04
Loam	0.044	0.081	2.806	1.237	0.77e-03
Silt	0.045	0.085	2.786	1.579	0.62e-03
Clay	0.000	0.056	3.070	0.182	0.20e-02
			Silt		
Sand	0.001	0.104	1.177	20.12	0.35e-01
Loam	0.001	0.028	1.250	1.040	0.57e-02
Silt loam	0.034	0.016	1.370	0.249	0.17e-04†
Clay	0.034	0.016	1.369	0.249	0.17e-04†
			Loam		
Sand	0.078	0.036	1.559	1.043	0.18e-04†
Sandy loam	0.078	0.036	1.559	1.042	0.18e-04†
Silt	0.078	0.036	1.559	1.042	0.18e-04†
Clay	0.078	0.036	1.559	1.042	0.18e-04†

*See Table 1.

†Optimized parameters are within 1% of true parameter values (Table 1).

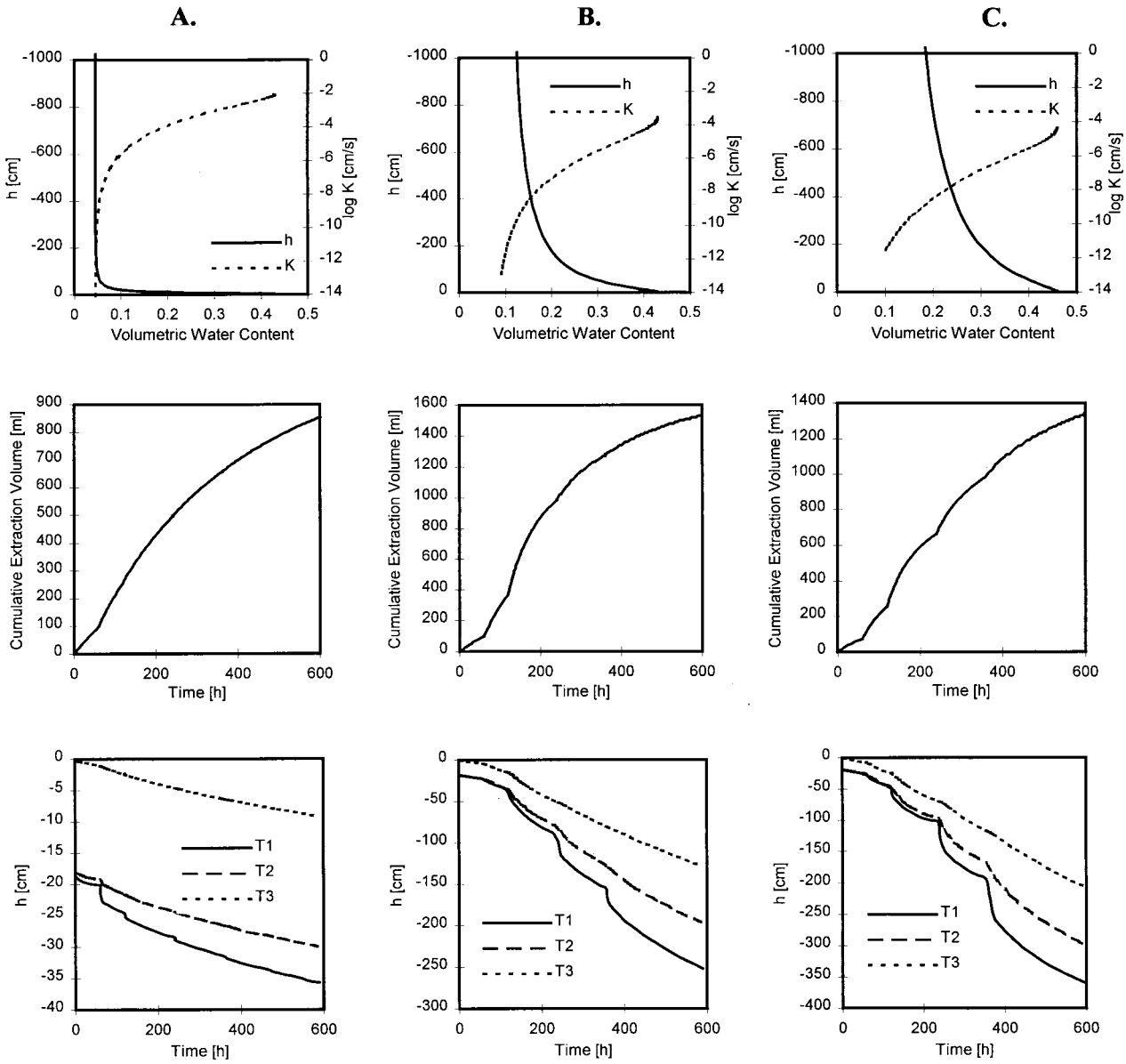

Figure 4. Soil water retention and unsaturated hydraulic conductivity curves with corresponding cumulative extraction volume (Q) and soil matric potential values (h) for (a) sand, (b) loam, and (c) silt as a function of time during multistep extraction (T_1, T_2, and T_3 represent tensiometers located at $(r, z) = (4, 18$ cm), (6, 18), and (6, 0.3), respectively; h, retention curve; K, hydraulic conductivity function).

the OF close to that of the global minimum. Consequently, the optimized parameter set is nonunique and could be far from the real set. This was particular true for the optimization results of the sandy soil. The true hydraulic functions with the corresponding simulated cumulative extraction volume (Q) and water potential head values (h_1, h_2, and h_3) are shown in Figure 4 for all three investigated soils.

Although the last applied vacuum step for the sandy soil is -480 cm, corresponding soil matric potential values do not decrease beyond -35 cm (Figure 4a), even at only 1-cm distance from the extraction device (T_1). Presumably, as the soil is near θ_r at this water potential, the soil's hydraulic conductivity becomes the limiting factor and much longer extraction experiments would be needed to yield information for water potential values smaller than -35 cm. Consequently, the optimized parameter values describe the hydraulic functions in the limited range of $-35 < h < 0$ cm only, with their shape largely controlled by the parameter n in the region. Inspection of Tables 1 and 2 shows that all optimized n and θ_r values are close to their real values of 2.68 and 0.045, respectively. Under these hypothetical experimental conditions, the parameters K_s and α appear insensitive to the OF, which can be concluded from the good fit (OF $< 10^{-2}$ in Table 2) for a wide range of values of these two parameters. Incidentally, the small changes in water potential values in both space and time will require highly accurate soil water potential measurements. Both Q and h_i ($i = 1, 2, 3$) responded weakly to the incremental changes in applied vacuum. The stepwise changes in vacuum were much more clearly evident in the extraction volume and soil matric potential responses for the other two soil types, where the drop of K with matric potential (h) is much smaller than for the sand (Figure 4).

Optimization results were slightly more successful for the silt soil (Figure 4c), for which two optimizations (using silt loam and clay initial parameters) converged to the true solution. Again, it is clear that n is the most sensitive parameter and K_s is the least sensitive parameter. In either case the choice of initial parameters is crucial to obtain convergence to the true parameter values. The best results were obtained for the loam soil (Figure 4b), for which convergence was achieved for any of the four sets of initial parameter values. As Figure 4b demonstrates, soil water retention of the loam is steadily decreasing over the range of 0 to -400 cm, whereas the rate of decrease in unsaturated K with water content is sufficient to cause a clear response of Q and h by step wise changes in applied vacuum. Both of these characteristics make the extraction method well suited for loamy-type soils under the given experimental conditions.

While reducing the number of optimized parameters to three by fixing θ_r to its true value, none of the sandy soil optimizations converged, whereas all the silt and loam optimizations converged to the true parameter values. These results show that reducing the number of free parameters increases uniqueness of the optimization problem, but at the same time can lead to ill-posed conditions. The results in Table 2 also show that the magnitude of the optimized K_s is proportional to α. Intuitively, this is clear as large α values correspond with coarser-textured soils of larger K_s.

Parameter sensitivity for soil matric potential and extraction volume measurements and the dependence of parameter sensitivity on tensiometer position were determined for all parameters using (11) and (13). Sensitivity of the measurement type is optimal for maximum $|s|$ values, and differences in sensitivity between parameters can be determined directly from comparison of s values. When comparing sensitivities to different parameters, one should recognize that the effect of a 1% change in one parameter of the soil hydraulic functions could be much different from that of the same 1% change of another parameter. *Šimunek and van Genuchten* [1996] showed that if the sensitivity of matric potential is estimated as a function of time during infiltration, parameter sensitivity is maximum when the time rate of change of soil matric potential is high. For suction infiltrometer measurements this occurred when the wetting front passed the depth of the tensiometer location. It is therefore anticipated that the sensitivity of soil matric potential measurements will increase using step increments in vacuum (multistep extraction) rather than using a single vacuum step, since a multitude of vacuum increments create a series of periods with increased soil matric potential gradients near the extraction device. Figure 5 shows the sensitivity (s) (Equation (11)) of soil matric potential (h_2) at T_2 (Figure 2) and cumulative extraction volume (Q) as a function of time for all optimized parameters for the loamy soil. When correcting for differences in absolute magnitude between Q and h, it becomes clear that the sensitivity of Q to any of the listed parameters is at least 5 times as large than the sensitivity of h. Figure 5 demonstrates that both cumulative extraction volumes and matric potentials are most sensitive to parameters α and n and least sensitive to θ_r and K_{cer}. Since K_s, contrary to parameters α and n, can change several orders of magnitude, the sensitivity to its value is significant as well. Moreover, Figure 5 shows that the sensitivity to all parameters increases with time.

Since the sensitivity is related to the time-rate of change of the measured flow variable, it is expected that the largest time-averaged sensitivity (S) in (13a) be at the interface of the extraction device and the soil. However, this is not completely so since the applied vacuum solely controls soil matric potential at that interface. In all, we find that the maximum sensitivity is near the extractor-soil interface and that sensitivity decreases as the tensiometer is positioned at larger distances from the extractor (loam and sand). However, in some cases (silt), sensitivity was high in the whole upper part of the flow domain, which was attributed to the limited size of the flow domain. In this part of the flow domain, soil matric potential changes are partly caused by the zero flux boundary condition, rather than by the applied vacuum in the extractor. The spatial distribution of the time-averaged sensitivity of n is shown in Figure 6 for each of the three soils.

Table 3 presents the time average and maximum sensitivity for all four parameters and three soil types. As was already anticipated from analysis of the parameter estimations, the parameter n is the most sensitive to the soil matric potential data, and K_s and θ_r are the least sensitive. Surprising, however, is the overall low sensitivity of all parameters for the loam relative to that of the silt and sand, when considering the excellent parameter optimization results of the loamy soil (Table 2). Sensitivity, as calculated by (13), reflects the behavior of the objective function in the vicinity of the true parameter values, that is, near the global minimum. Therefore higher sensitivity means that the minimum is better defined and should be estimated with higher precision once the global minimum is identified. It does not, however, give any information about the other possible local minima in the objective function (e.g., for sand and silt) elsewhere in the entire parameter space.

3.2. Laboratory Experiment

The parameters of the soil hydraulic functions were optimized using the multistep extraction laboratory experiment. Three sets of initial parameter values were arbitrarily selected from Table 1. For each set of optimizations, Table 4 includes the optimized parameter values as well as their uncertainty. The latter is determined from the main diagonal of the parameter covariance matrix, and is expressed by the normalized standard deviation (NSD), equal to the ratio of standard deviation and optimized parameter value. In this manner the uncertainties of the parameters can be evaluated by direct comparison of the NSD values. The objective function for this experiment included the water volume measurements at t_0 and t_{end}, in addition to cumulative extraction volume and the matric potential values at the three tensiometer locations. Since no saturated water content value (θ_s) was available, its value was also optimized, bringing the total number of optimized parameters to five. However, since the volume of water present at t_0 was known and included in the OF, optimization of θ_s did not compromise the numerical inversion. For the first set of optimizations ("fixed K_{cer}"), the measured value of the ceramic conductivity, K_{cer}, was taken as a fixed parameter in the optimization. The results of the optimizations are presented in Figures 7a and 7b, and the corresponding optimized parameter values are listed in Table 4. The contributions of cumulative extraction volume, soil matric potential at three positions combined, and soil water storage to the total value of the OF are listed separately in Table 5.

We obtained very good agreement between measured and calculated cumulative extraction volumes for the fixed K_{cer} case (Figure 7a). However, it is apparent from Figure 7b that

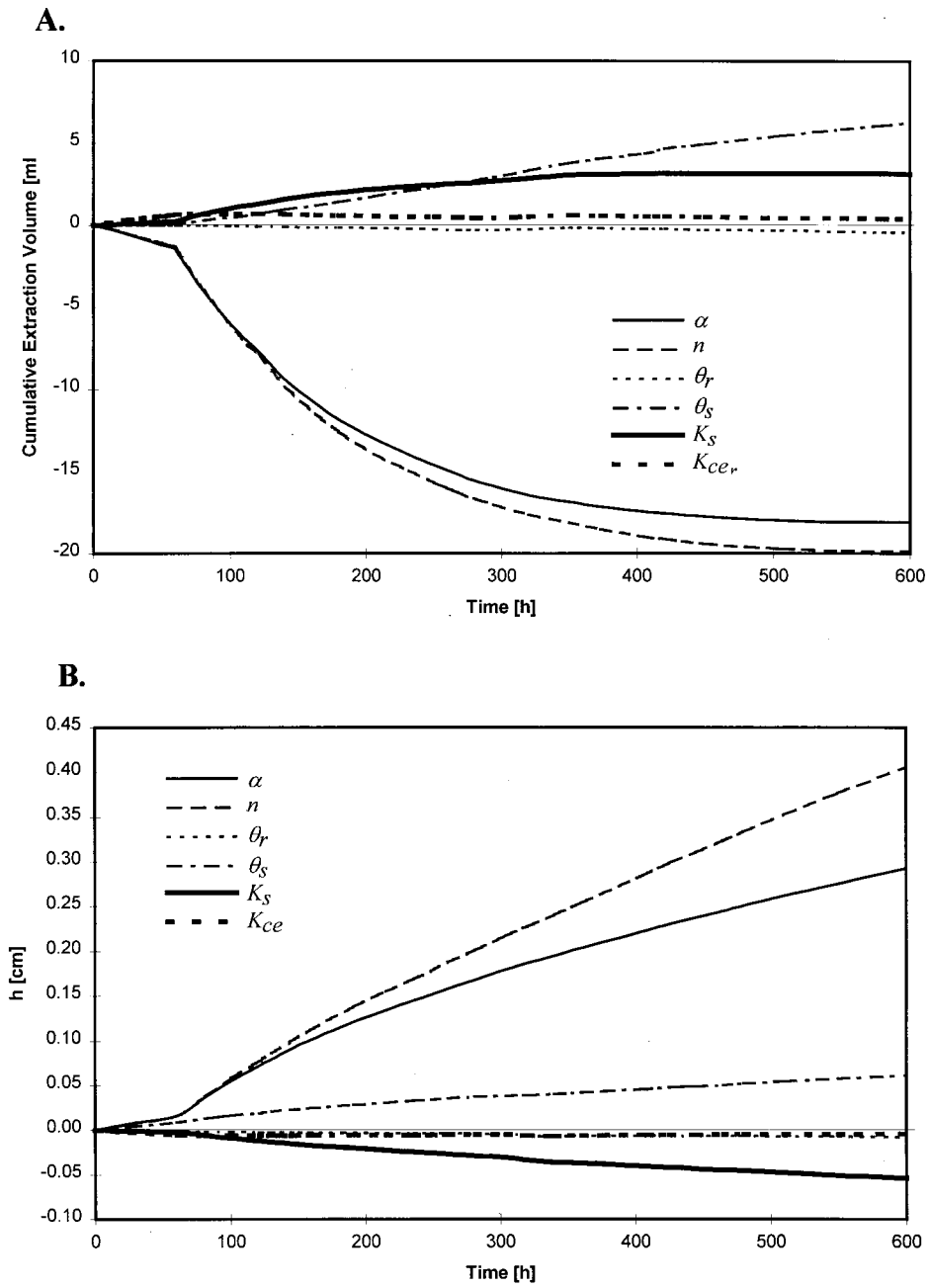

Figure 5. Sensitivity ($s_{i,j}$) of (a) cumulative extraction volume (Q) and (b) soil matric potential values (h_2) to the parameters θ_r, θ_s, α, n, K_s, and K_{cer} as a function of time for loamy soil.

the optimized soil water potential values do not match the corresponding measured values well. We hypothesized that the independently measured K_{cer} was not representative for the experimental conditions because of imperfect hydraulic contact between the ceramic and the surrounding soil. Since it is impossible to estimate the contact area, K_{cer} was also included as a free parameter to be optimized. The results of these optimizations are listed as "fitted K_{cer}" in Table 4. Instead of the measured value of 0.000834 cm h^{-1}, its optimized value was only 0.00025 cm h^{-1}. As a result of including K_{cer} as an additional free parameter, the value of the OF (equation (9)) decreased from 0.0753 to 0.0503 (Table 5), and parameter uncertainty as expressed by NSD (Table 4) was reduced. However, the overall decrease in deviations in the OF was at the expense of an increase in deviations between measured and optimized cumulative extraction volume (see first column of Table 5) and between measured and optimized soil matric potential values for the first three vacuum steps. Consequently, for the third set of optimizations, it was assumed that K_{cer} was equal to the measured value of 0.000834 cm h^{-1} for the first three vacuum increments (hydraulic contact is assumed to be perfect) but decreased thereafter to a value to be optimized as hydraulic contact decreases because of soil desaturation. The results of these optimizations ("variable K_{cer}") are shown in Figures 7c and 7d, and in the last column of Table 4. Convergence was obtained with K_{cer} = 0.00013 cm h^{-1}, corresponding with a further decrease of parameter uncertainty (Table 4) and of the OF from 0.0503 to 0.0184 (Table 5). Although the

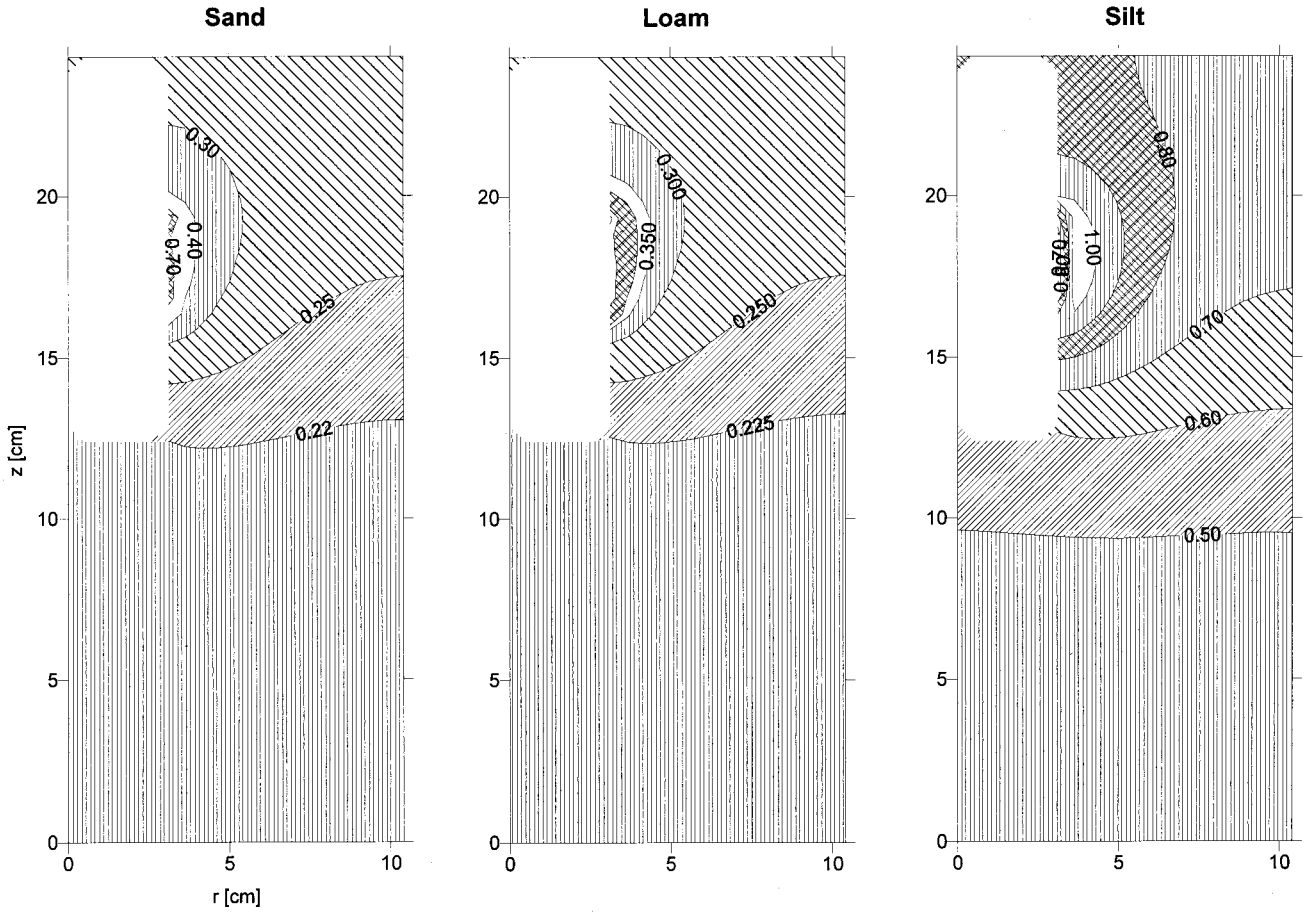

Figure 6. Contour plots of time-averaged sensitivity ($S(r, z, b_j)$) of the soil matric potential to the parameter n of multistep extraction experiment for all three soils.

cumulative extraction volume fit is not as good as for the first case with a fixed ceramic conductivity (compare Figures 7a and 7c), an excellent fit was obtained for the soil matric potential data for all but the last vacuum increment. Comparison of the three cases in Table 4 shows that the increase in the optimized K_s value compensates for the corresponding reduction in K_{cer}. Thus the reduction in hydraulic contact area is artificially compensated for in the simulations by a decrease in the optimized soil's saturated hydraulic conductivity.

Close inspection of Table 5 shows that the type of weighting employed in our optimizations results in OF values that are dominated by soil matric potential measurements (72–98% of total OF value). However, it is not very clear how differences in weighting affects the OF value. For example, it is expected that deviations in soil matric potential values will increase if measurement or model errors are larger. Although we have some knowledge about measurement errors, the magnitude of the model error and its contribution to the OF is unknown. Also, soil heterogeneity will increase deviations between measured and simulated soil water potential values (point measurements) since the model assumes a homogeneous soil, whereas cumulative extraction volume (whole domain measurement) is not affected by soil heterogeneity.

Table 4 also lists the soil hydraulic parameters obtained independently by multistep outflow method with one tensiometer in the center of the core [*Eching and Hopmans*, 1993]. These were obtained by fitting core-average retention points to the van Genuchten function (6). Estimated soil hydraulic functions for all three optimization options (fixed K_{cer}, fitted K_{cer}, and variable K_{cer}) together with those determined independently are shown in Figure 8. The best agreement of the presented optimizations with the independently determined soil hydraulic functions was achieved using the variable K_{cer} optimization option. The difference in K_s between the variable K_{cer} case and the independently estimated hydraulic functions is about 1 order in magnitude (0.327 versus 4.2 cm h^{-1}), whereas the other parameter values, especially the shape parameters α and n, are relatively close.

3.3. Field Experiment

The selected diameter of the radial-symmetric computational domain for the field experiment was 70 cm. The domain

Table 3. Time-Averaged Sensitivity and Maximum Sensitivity of Soil Matric Potential to a 1% Change of the Parameters θ_r, α, n, and K_s for the sand, silt, and loam

Soil Type	Sensitivity S			
	θ_r	α	n	K_s
Sand	0.04 (0.093)	0.425 (1.96)	1.08 (3.04)	0.075 (0.344)
Silt	0.42 (0.088)	1.180 (2.74)	1.06 (2.15)	0.422 (1.029)
Loam	0.067 (0.493)	0.429 (1.51)	1.083 (2.28)	0.108 (0.660)

Maximum sensitivity given in parentheses.

Table 4. Parameter Estimation Results for Laboratory Experiment

Parameter	Fixed K_{cer}		Fitted K_{cer}		Variable K_{cer}		Columbia Sandy Loam, Independently Measured
	Value	NSD, %	Value	NSD, %	Value	NSD, %	
α, cm^{-1}	0.00596	4.2	0.00738	3.5	0.0077	1.4	0.0093
n	2.219	6.2	2.706	5.8	3.143	3.7	3.26
θ_s	0.37	0.1	0.370	0.07	0.37	0.04	0.43
θ_r	0.100	16.7	0.176	4.3	0.197	1.3	0.14
K_s, cm h^{-1}	0.0262	15.5	0.129	24.4	0.393	19.3	4.2
K_{cer}, cm h^{-1}	0.000834	···	0.00025	7.9	0.00013	7.7	···

NSD, normalized standard deviation, $100\sigma/b_j$ (%), estimated from parameter variance.

size was large to justify the assumption of a zero flux boundary condition along the lateral boundaries. The size of the domain for which zero lateral flux can be assumed will depend on soil type. It can be relatively small for sandy soils for which the fast decrease in unsaturated hydraulic conductivity with increased suction along the extraction device limits the size of the domain of influence but must be larger for loamy and clayey soils.

The measured decrease in soil water potential at the lower boundary of the simulated soil domain (T_4) from the time that internal drainage start (t_0) was fitted with the following power function:

$$h_{lb} = a(t + b)^c + d \tag{15}$$

The fitted power function through the measured soil water potential data of the 55-cm-depth tensiometer is used as lower boundary condition (h_{lb}) for the flow simulation. Fitted values for the coefficients were: $a = -62.1$, $b = 0.772$, $c = 0.147$, and $d = 45.9$, where time (t) and soil water potential (h_{lb})

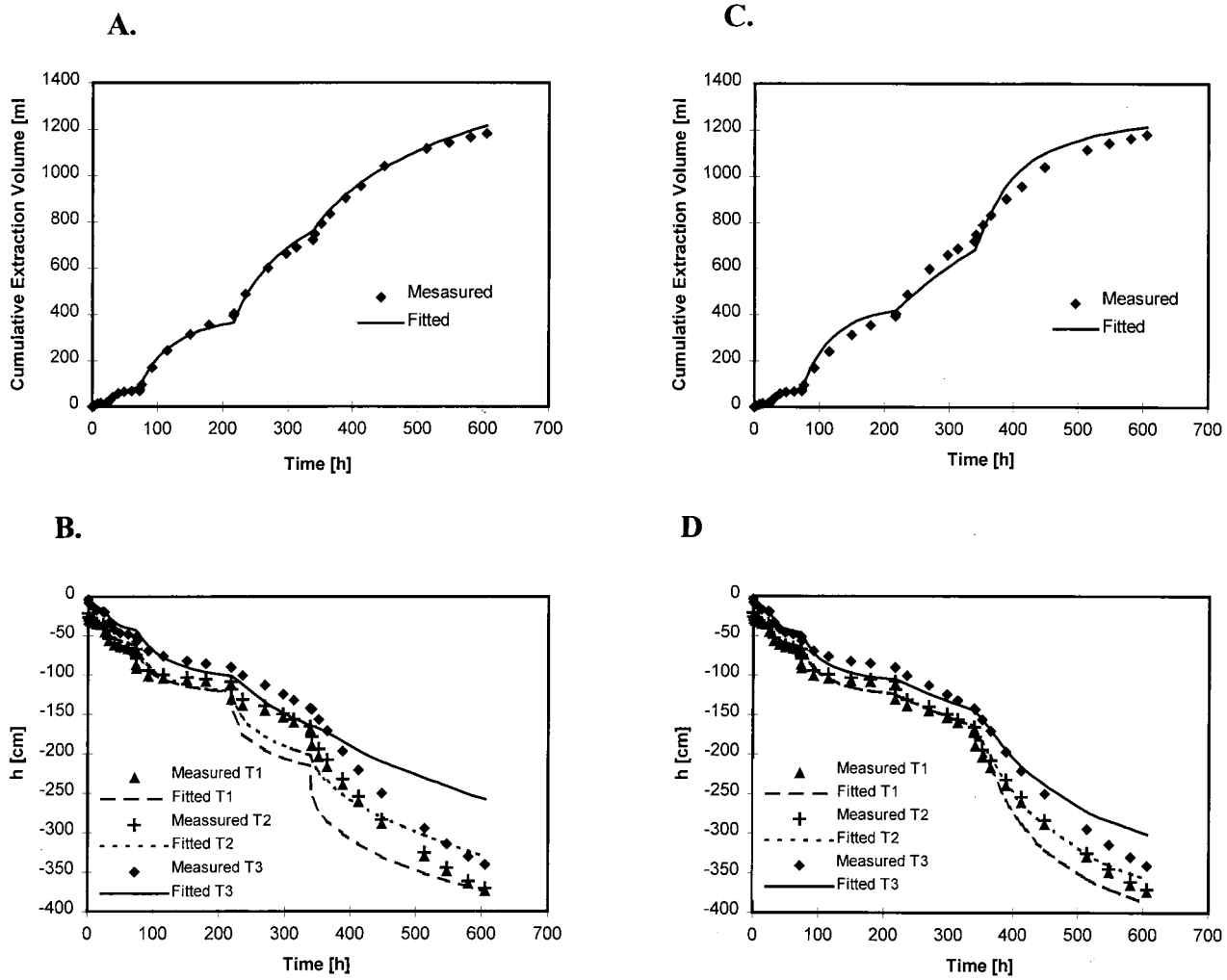

Figure 7. Comparison of measured (symbols) and optimized (lines) cumulative extraction (Q) and soil matric potential values (h) using (a, b) a fixed K_{cer} value and (c, d) optimized K_{cer} ("variable K_{cer}"). Laboratory experiment.

Table 5. Contribution of Measurement Type to OF for Laboratory Experiment

Case	Contribution to OF			Total OF
	Q	h_i, $i = 1, 2, 3$	Water Storage	
Fixed K_{cer}	0.0013	0.0741	0.71e-07	0.0753
Fitted K_{cer}	0.0124	0.0379	0.986e-05	0.0503
Variable K_{cer}	0.0052	0.0132	0.129e-04	0.0184

are given in hours and cm, respectively. The value for h_{lb} at t_0 was -13.9 cm. The measured hydraulic head gradient of 1.0 cm/cm was used to estimate $h_i(z)$ at time t_0. The data points in Figure 9 correspond with the measured soil matric potential values and cumulative extraction volume after infiltration stopped and internal drainage started ($t_0 = 0$), with the first vacuum step applied after $t = 46.5$ h after which soil water was extracted. Soil water potential values showed little response to vacuum increments, except for the tensiometer (T_1), which was positioned 1 cm from the extraction device. The jumps in T_1 values correspond with the applied vacuum increments.

The soil water extractor was the same as used in the laboratory experiments with a measured K_{cer} value of 0.0008334 cm h^{-1}. However parameter optimizations using this value were not very successful with relatively large differences between optimized and measured extraction volume and soil water potential values. Hence the same approach as in the laboratory was used, allowing K_{cer} to be optimized. The final results are shown in Figures 9a and 9b, with the optimized parameter values listed in Table 6 (fitted K_{cer}). Using a K_{cer} of 0.000282, the fit for the field experiment was extremely good (Figures 9a and 9b), reducing the OF value with a factor of 6 (Table 6). From the information included into the objective function, that is, the cumulative extracted volume and tensiometer readings, it is not possible to estimate simultaneously both θ_r and θ_s, since these two parameters are fully correlated. It is possible either to fix one of these two parameters and to optimize the other or to optimize the water content interval $\Delta\theta = \theta_s - \theta_r$. Both approaches should result in similar results. We fixed θ_s at the independently measured value (0.560) and estimated θ_r. Note from the parameter estimation results given in Table 6 that the water content interval $\Delta\theta$ was small and equal to only 0.120 $cm^3\ cm^{-3}$. The water content interval between the initial water content and the water content corresponding to the measured soil matric potential value at T_1 must have a close correspondence with the cumulative extracted volume. The small value of $\Delta\theta$ was the result of the relatively small amount of water extracted during the experiment (only about 0.5 L). The results in Table 6 also show the large uncertainty of the saturated hydraulic conductivity K_s for which the value of NSD is always larger than 60%.

The reduction of the optimized against measured hydraulic conductivities of the ceramic cylinder, K_{cer}, is similar for both laboratory and field experiments. The ratio between optimized K_{cer} and K_{cer} measured independently is 0.30 and 0.34 for the laboratory and field experiments, respectively. K_{cer} measurements were carried out while the ceramic was fully submerged in water. When similar measurements were performed in conductive saturated sand, the measured K_{cer} was significantly lower (0.000560 versus 0.0008334 cm h^{-1}).

In addition to cumulative extraction volume and soil matric potential values at three locations, we also included the three independently measured $\theta(h)$ points during the extraction experiment in the objective function. Inclusion of such information into the objective function breaks the mutual correlation of θ_r and θ_s so that now both parameters can be estimated simultaneously. Figures 9c and 9d show the comparison between measured and calculated cumulative extraction volumes and tensiometer readings, respectively. The fit of experimental with fitted cumulative extraction volumes and matric potential values for T_2 and T_3 is similar to those for the previous optimizations (Figures 9a and 9b). However, deviations between measured and fitted matric potential data for T_1 increased in the final extraction step.

Figure 10 presents the optimized soil water retention and hydraulic conductivity functions for the fitted K_{cer} case with and without the independently determined $\theta(h)$ data, as well as the soil hydraulic data estimated independently by the in-

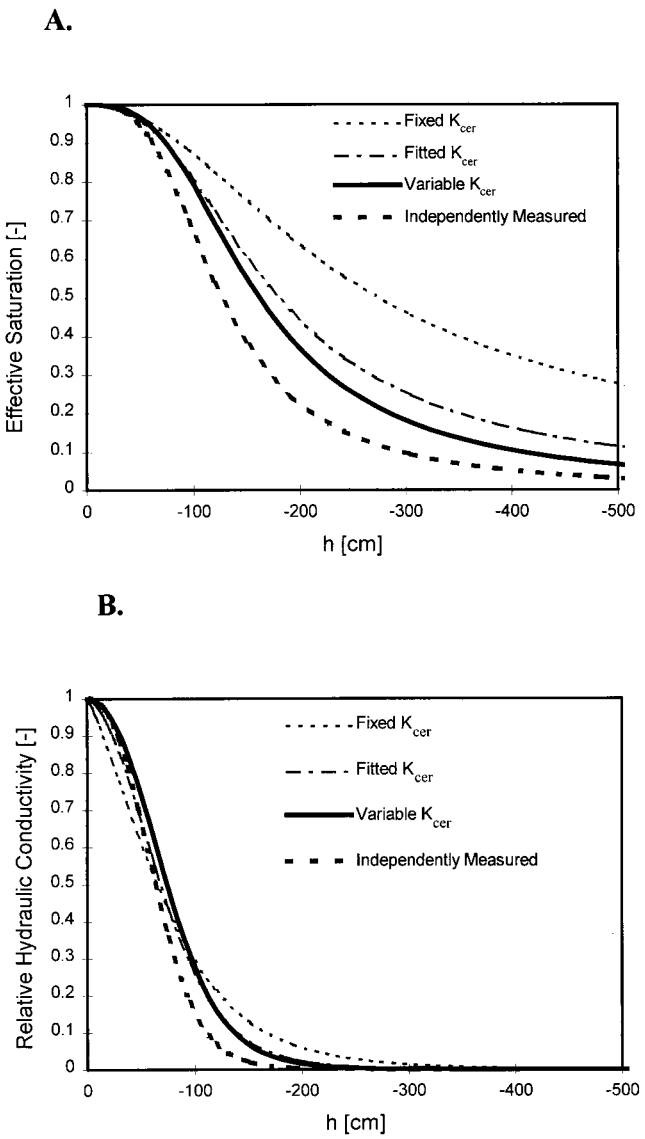

Figure 8. (a) Estimated soil water retention and (b) hydraulic conductivity functions for three optimization options (Table 4) for Columbia sandy loam, compared with independently determined curves.

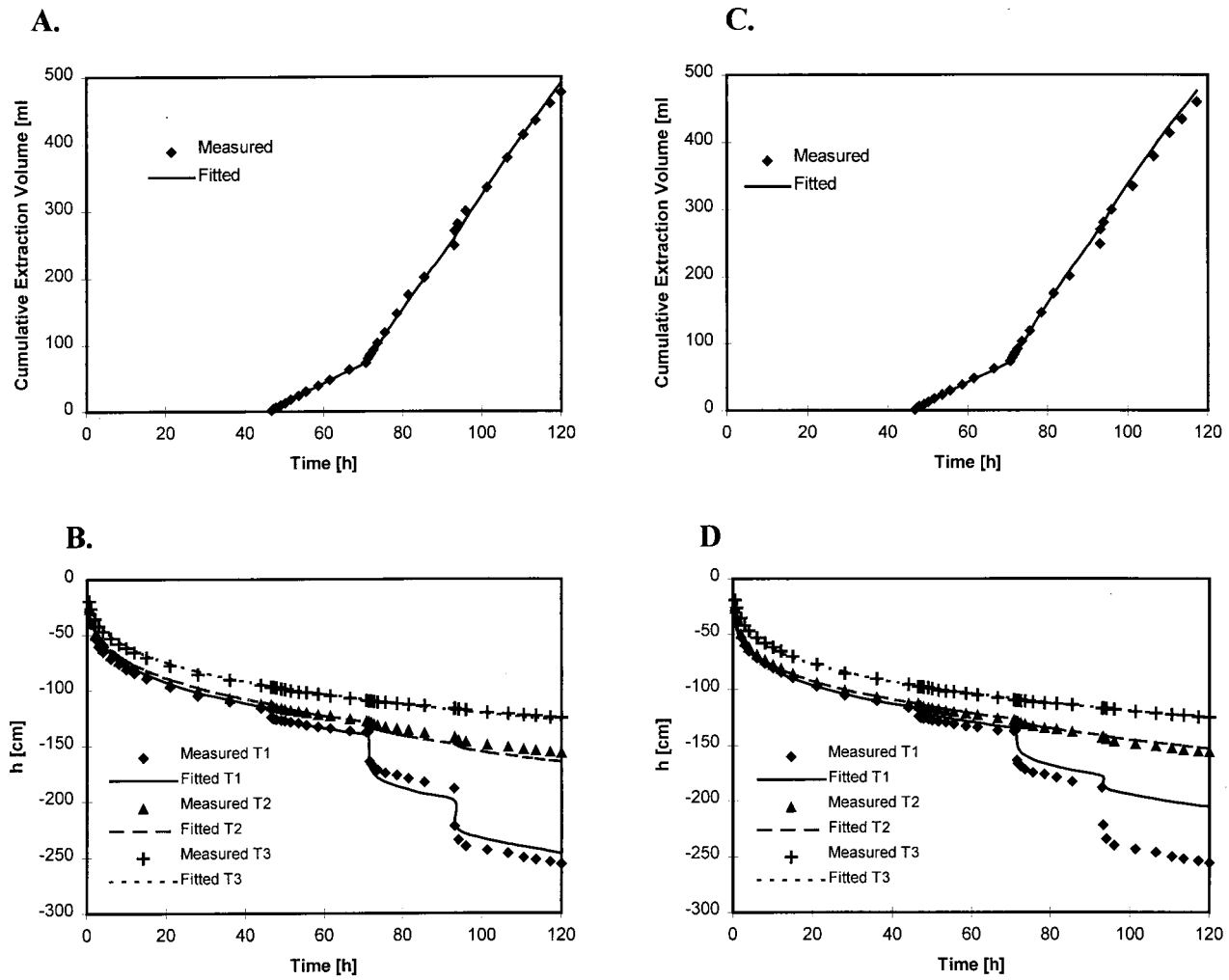

Figure 9. Comparison of measured (symbols) and optimized (lines) cumulative extraction and soil matric potential values (h) using an optimized K_{cer} value. Objective function includes (a), (b) cumulative extraction volumes and soil matric potential measurements and (c), (d) three measured $\theta(h)$ data points. Field experiment.

stantaneous profile method (diamond symbols). Figure 10a also includes the three $\theta(h)$ points (solid circles). Both optimized soil water retention and unsaturated hydraulic conductivity functions closely approximate the independently estimated retention and unsaturated hydraulic conductivity data in the range between -150 and -50 cm. However, the optimized parameters and hydraulic functions are only valid for the soil matric potential range from near saturation to about -250 cm, that is, the range over which the extraction experiment was carried out. Continued soil water extraction after 5 days would have generated soil matric potential data smaller than measured in the described field experiment.

4. Summary and Conclusions

We have introduced a new method for estimating soil hydraulic parameters from a transient flow experiment. The experiment involves extraction of soil solution using successively

Table 6. Parameter Estimation Results for Field Experiment

	Fixed K_{cer}		Fitted K_{cer}		Fitted K_{cer} + $\theta(h)$ data	
Parameter	Value	NSD, %	Value	NSD, %	Value	NSD, %
α, cm^{-1}	0.0331	18.3	0.0231	23.4	0.0220	30.0
n	1.746	2.6	1.688	2.2	2.313	6.0
θ_s	0.560	···	0.560	···	0.552	11.9
θ_r	0.389	3.43	0.441	3.34	0.301	1.3
K_s, cm h^{-1}	8.932	62.4	3.28	74.4	9.725	119.8
K_{cer}, cm h^{-1}	0.0008334	···	0.000282	3.5	0.00026	3.9
OF(**b**)	0.0686	···	0.0109	···	0.0787	···

NSD, normalized standard deviation, $100\sigma/b_j$ (%), estimated from parameter variance.

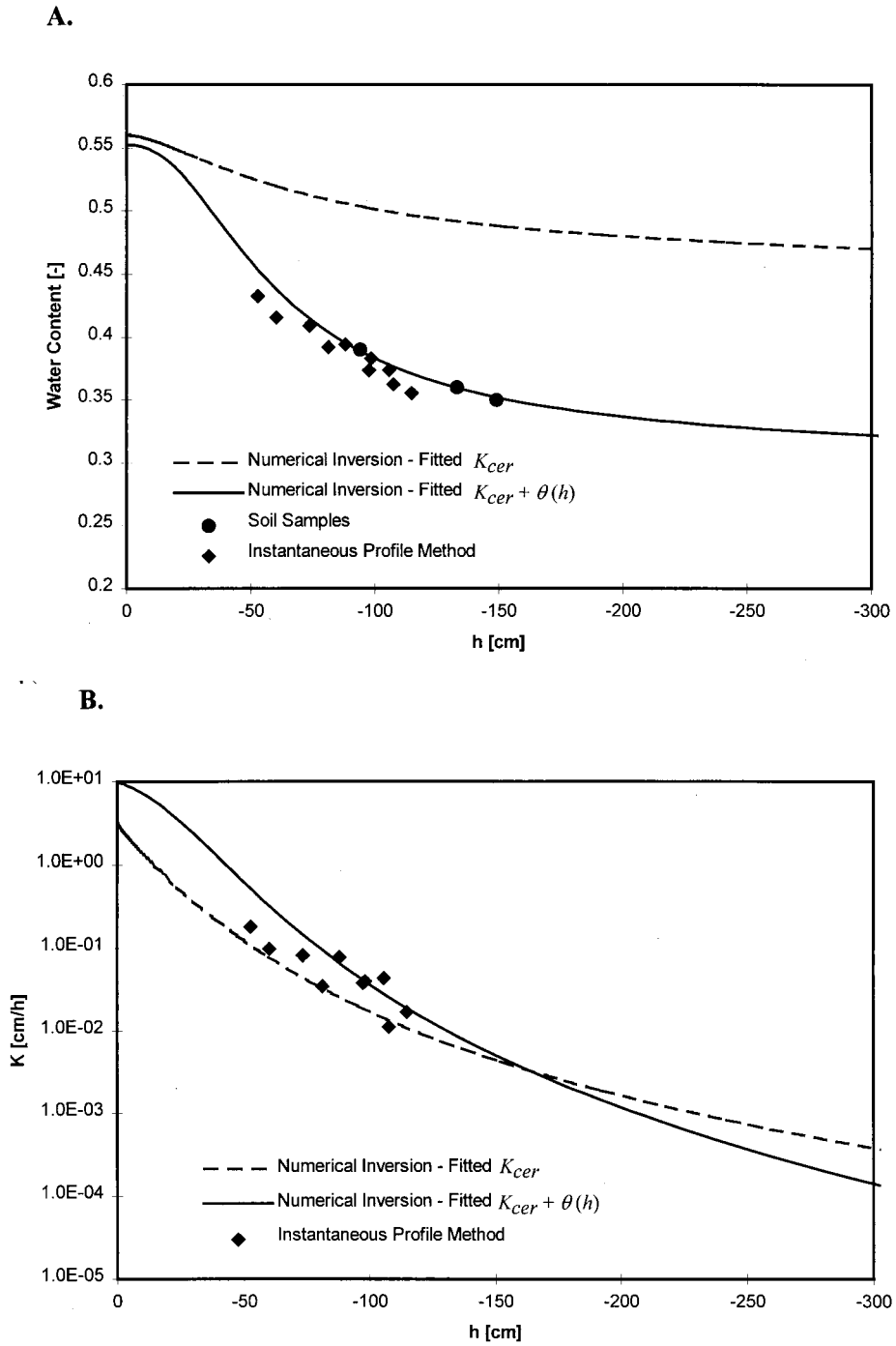

Figure 10. (a) Estimated soil water retention and (b) hydraulic conductivity functions for the two optimization options of Table 6 for Yolo clay loam, compared with independently determined retention and unsaturated hydraulic conductivity data.

increasing vacuum steps from an initially near-saturated soil. The extracted volume and measured soil matric potential values at several locations near the soil water extraction device are measured. The collected data are analyzed by a numerical code, which combines the Levenberg-Marquardt optimization algorithm with the unsaturated water flow code HYDRUS-2D. The soil hydraulic parameters are obtained by minimization of the objective function, which includes the deviations between simulated and experimental data.

We evaluated the feasibility of the vacuum extraction technique using numerically generated data. We concluded that the method is well suited for loamy-textured soils but not for sandy soils. This is because the matric potential response to the applied vacuum in the sandy soil is minimal. The success of the inversion procedure for the silt soil is dependent on initial parameter values. Parameter sensitivity analysis showed that the method is most sensitive to the shape parameters α and n and least sensitive to the residual water content θ_r and the

saturated hydraulic conductivity K_s. The highest sensitivity of the measured soil matric potential head is close to the extraction device and decreases with increasing distance from the extractor. Therefore tensiometers should be located close to the ceramic ring where the extraction vacuum is applied.

The method was further tested under well-defined experimental conditions in a laboratory for a Columbia sandy loam. The objective function included the cumulative extraction volume, soil matric potential readings for three tensiometers, and the initial and final total water volumes in the soil sample. Parameter optimization was successful if the saturated hydraulic conductivity of the extractor (K_{cer}) was optimized simultaneously with the soil hydraulic parameters rather than assuming its independently measured value. We hypothesize that K_{cer} is changing during the extraction experiment because of reduction of hydraulic contact between the ceramic ring and the surrounding soil as the soil desaturates.

Finally, the multistep extraction method was tested in situ for a Yolo silt loam. Optimized soil water retention and unsaturated hydraulic conductivity data corresponded well with independent estimates obtained from the instantaneous profile method in the same experimental plot. However, care should be taken in extrapolating the optimized hydraulic functions beyond the water content range for which the experimental data were obtained.

The problem of hydraulic contact between the ceramic membrane and the surrounding soil is of critical importance for further applications of the extraction method. From our analysis it appears that although we took great care to assure hydraulic contact when installing the extraction device, hydraulic contact was reduced during soil water extraction, thereby affecting the optimization results. To overcome this problem, improved devices such as those presented by *Shani and Or* [1995], which guarantee hydraulic contact with the surrounding soil throughout the duration of the extraction experiment, need to be developed. Moreover, similar to the experiments by *Gribb* [1996], the experimental procedure would be greatly simplified if the tensiometers and extraction device were combined into a single probe.

Acknowledgments. This research was supported by a grant from the Water Resources Center. We thank Jim MacIntyre for his tireless work assisting in the experimental part of the study. We also acknowledge Rien van Genuchten of the USDA-ARS Salinity Laboratory for his support. The authors also thank Brent Clothier and another anonymous reviewer for their constructive criticism.

References

Bard, Y., *Nonlinear Parameter Estimation*, 341 pp., Academic, San Diego, Calif., 1974.

Brooks, R. H., and A. T. Corey, Properties of porous media affecting fluid flow, *J. Irrig. Drain. Div. Am. Soc. Civ. Eng.*, *92*, 61–88, 1966.

Carrera, J., and S. P. Neuman, Estimation of aquifer parameters under transient and steady state conditions, 1, Maximum likelihood method incorporating prior information, *Water Resour. Res.*, *22*, 199–210, 1986a.

Carrera, J., and S. P. Neuman, Estimation of aquifer parameters under transient and steady state conditions, 2, Uniqueness, stability, and solution algorithms, *Water Resour. Res.*, *22*, 211–227, 1986b.

Carsel, R. F., and R. S. Parrish, Developing joint probability distributions of soil water retention characteristics, *Water Resour. Res.*, *24*(5), 755–769, 1988.

Celia, M. A., E. T. Bouloutas, and R. L. Zarba, A general mass-conservative numerical solution for the unsaturated flow equation, *Water Resour. Res.*, *26*(7), 1483–1496, 1990.

Clausnitzer, V., and J. W. Hopmans, Non-linear parameter estimation: LM_OPT. General-purpose optimization code based on the Levenberg-Marquardt algorithm, *Land*, *Air Water Resour. Pap. 100032*, Univ. of Calif., Davis, 1995.

Dirksen, C., Unsaturated hydraulic conductivity, in *Soil Analysis: Physical Methods*, edited by K. A. Smith and C. E. Mullins, pp. 209–269, Marcel Dekker, New York, 1991.

Doering, E. J., Soil water diffusivity by the one-step method, *Soil Sci.*, *99*, 322–326, 1965.

Eching, S. O., and J. W. Hopmans, Optimization of hydraulic functions from transient outflow and soil water pressure data, *Soil Sci. Soc. Am. J.*, *57*(5), 1167–1175, 1993.

Eching, S. O., J. W. Hopmans, and O. Wendroth, Unsaturated hydraulic conductivity from transient multi-step outflow and soil water pressure data, *Soil Sci. Soc. Am. J.*, *58*, 687–695, 1994.

Gardner, W. R., Calculation of capillary conductivity from pressure plate outflow data, *Soil Sci. Soc. Am. Proc.*, *20*, 317–320, 1956.

Green, R. E., L. R. Ahuja, and S. K. Chong, Hydraulic conductivity, diffusivity, and sorptivity of unsaturated soils: field methods, in *Methods of Soil Analysis*, part I, monogr. 9, edited by A. Klute, 2nd ed., pp. 771–798, Soil Sci. Soc. of Am., Madison, Wis., 1986.

Gribb, M. M., Parameter estimation for determining hydraulic properties of a fine sand from transient flow measurements, *Water Resour. Res.*, *32*(7), 1965–1974, 1996.

Klute, A., Water retention: Laboratory methods, in *Methods of Soil Analysis*, part I, monogr. 9, edited by A. Klute, 2nd ed., pp. 635–662, Soil Sci. Soc. of Am., Madison, Wis., 1986.

Klute, A., and C. Dirksen, Conductivities and diffusivities of unsaturated soils, in *Methods of Soil Analysis*, part I, monogr. 9, edited by A. Klute, 2nd ed., pp. 687–734, Soil Sci. Soc. of Am., Madison, Wis., 1986.

Kool, J. B., and J. C. Parker, Analysis of the inverse problem for transient unsaturated flow, *Water Resour. Res.*, *24*(6), 817–830, 1988.

Kool, J. B., J. C. Parker, and M. T. van Genuchten, Determining soil hydraulic properties for one-step outflow experiments by parameter estimation, I, Theory and numerical studies, *Soil Sci. Soc. Am. J.*, *49*, 1348–1354, 1985.

Kool, J. B., J. C. Parker, and M. T. van Genuchten, Parameter estimation for unsaturated flow and transport models—A review, *J. Hydrol.*, *91*, 255–293, 1987.

Marquardt, D. W., An algorithm for least-squares estimation of nonlinear parameters, *SIAM J. Appl. Math.*, *11*, 431–441, 1963.

Mualem, Y., A new model for predicting the hydraulic conductivity of unsaturated porous media, *Water Resour. Res.*, *12*, 513–522, 1976.

Parker, J. C., J. B. Kool, and M. T. van Genuchten, Determining soil hydraulic properties from one-step outflow experiments by parameter estimation, II, Experimental studies, *Soil Sci. Soc. Am. J.*, *49*, 1354–1359, 1985.

Shani, U., and D. Or., In situ method for estimating subsurface unsaturated hydraulic conductivity, *Water Resour. Res.*, *31*, 1863–1870, 1995.

Šimunek, J., and M. T. van Genuchten, Estimating unsaturated soil hydraulic properties from tension disc infiltrometer data by numerical inversion, *Water Resour. Res.*, *32*(9), 2683–2696, 1996.

Šimunek, J., and M. T. van Genuchten, Parameter estimation of soil hydraulic properties from multiple tension disc infiltrometer data, *Soil Sci.*, *6*, 383–398, 1997.

Šimunek, J., M. Sejna, and M. T. van Genuchten, The HYDRUS-2D software package for simulating water flow and solute transport in two-dimensional variably saturated media, version 1.0, *IGWMC-TPS-53*, Int. Ground Water Modeling Cent., Colo. School of Mines, Golden, 1996.

Toorman, A. F., P. J. Wierenga, and R. G. Hills, Parameter estimation of soil hydraulic properties from one-step outflow data, *Water Resour. Res.*, *28*, 3021–3028, 1992.

Valiantzas, J. D., and D. G. Kerkides, A simple iterative method for the simultaneous determination of soil hydraulic properties from one-step outflow data, *Water Resour. Res.*, *26*, 143–152, 1990.

van Dam, J. C., J. N. M. Stricker, and P. Droogers, From one-step to multi-step determination of soil hydraulic functions by outflow experiments, *Rep. 7*, Dep. of Water Resour., Agric. Univ., Wageningen, Netherlands, 1990.

van Dam, J. C., J. N. M. Stricker, and P. Droogers, Inverse method for determining soil hydraulic functions from multi-step outflow experiments, *Soil Sci. Soc. Am. J.*, *58*, 647–652, 1994.

van Genuchten, M. T., A closed-form equation for predicting the

hydraulic conductivity of unsaturated soils, *Soil Sci. Soc. Am. J.*, *44*, 892–898, 1980.

Whisler, F. D., and K. K. Watson, One-dimensional gravity drainage of uniform columns of porous materials, *J. Hydrol.*, *6*, 277–296, 1968.

Yeh., W. W.-G., Review of parameter identification procedures in groundwater hydrology: The inverse problem, *Water Resour. Res.*, *22*(2), 95–108, 1986.

V. Clausnitzer and J. W. Hopmans, Hydrology Program, Dept. LAWR, University of California, Davis, CA 95616. (e-mail: jwhopmans@ucdavis.edu)

M. Inoue, Arid Land Research Center, Tottori University, Tottori, Japan.

J. Šimunek, USDA Salinity Laboratory, USDA-ARS, 450 Big Springs Road, Riverside, CA 92507.

(Received July 14, 1997; revised January 15, 1998; accepted January 22, 1998.)